# Nonintrusive Global Sensitivity Analysis for Linear Systems With Process Noise

**Souransu Nandi**
Control, Dynamics and Estimation Laboratory,
Department of Mechanical and
Aerospace Engineering,
University at Buffalo,
Buffalo, NY 14260
e-mail: souransu@buffalo.edu

**Tarunraj Singh**
Control, Dynamics and Estimation Laboratory,
Department of Mechanical
and Aerospace Engineering,
University at Buffalo,
Buffalo, NY 14260
e-mail: tsingh@buffalo.edu

*The focus of this paper is on the global sensitivity analysis (GSA) of linear systems with time-invariant model parameter uncertainties and driven by stochastic inputs. The Sobol' indices of the evolving mean and variance estimates of states are used to assess the impact of the time-invariant uncertain model parameters and the statistics of the stochastic input on the uncertainty of the output. Numerical results on two benchmark problems help illustrate that it is conceivable that parameters, which are not so significant in contributing to the uncertainty of the mean, can be extremely significant in contributing to the uncertainty of the variances. The paper uses a polynomial chaos (PC) approach to synthesize a surrogate probabilistic model of the stochastic system after using Lagrange interpolation polynomials (LIPs) as PC bases. The Sobol' indices are then directly evaluated from the PC coefficients. Although this concept is not new, a novel interpretation of stochastic collocation-based PC and intrusive PC is presented where they are shown to represent identical probabilistic models when the system under consideration is linear. This result now permits treating linear models as black boxes to develop intrusive PC surrogates.* [DOI: 10.1115/1.4041622]

## 1 Introduction

Integral to the task of forecasting is the uncertainty in initial conditions, model parameters, unmodeled dynamics, and stochastic disturbances. The Kalman filter [1] and its numerous derivatives such as the unscented transform filter [2], conjugate unscented transform filter [3], and ensemble Kalman filter [4,5] use the mean and covariance to quantify the uncertainty in the evolving states of a dynamic process. The typical source of uncertainty in a Kalman filter is process noise, which can represent unmodeled dynamics or stochastic input, and the uncertainty in the states is a function of the initial state uncertainty and the statistics of the stochastic input. Model parameter uncertainties are not typically included in characterizing the uncertainty in the forecast variables under the framework of the Kalman paradigm. In the presence of model parameter uncertainties, one is confronted with the question: how confident can one be in the estimate of the variance of the output resulting from the propagation of Kalman filters.

Whether the goal is evacuation in the face of an impending hurricane, grounding a high value asset for preventative maintenance, fault detection and isolation or avoiding expensive maneuvering of the space station to avoid the potential of collision with space debris, uncertainty in the state estimates is the bane of any decision maker. It is, therefore, not difficult to motivate the need to comprehend the impact of various sources of uncertainties on the uncertainty of the output of interest. This formal apportionment of uncertainty in the output to the various causal uncertain sources can permit identification of the subset of the uncertain sources that predominantly contribute to the uncertainty in the output. This is the purview of *global sensitivity analysis* (GSA), which has garnered increasing attention over the past two decades [6].

Global sensitivity analysis has been exploited by Cho et al. [7] where they submit that parameter sensitivity analysis can be used to provide guidance on which measurement to consider for better estimation of model parameters. This in essence is an efficient (optimal) design of experiments to maximize the accuracy of the estimation of model parameters [8].

Global sensitivity analysis can be used to exercise the spirit of Occam's Razor, which is an articulation of endorsing the simplest model. GSA can help identify variables, which have minimal to no impact on the output and can consequently be eliminated (or fixed) from the set of variables used to parameterize the model, i.e., help in model reduction [6].

Global sensitivity analysis has also been used to characterize contribution of uncertainty to outputs of interest, which vary over time [9–13]. Since this division of contribution keeps changing dynamically, it is often desired to know when the influence of an uncertain parameter is significant. For example, it is possible that a parameter is seen to be most significant during transients while its influence is minimal elsewhere in time. For applications where the steady-state operation is of interest, it might be then prudent to not invest resources in better estimating those parameters since their influence is minimal at the time of interest. McRae et al. [12] (where the popular Fourier amplitude sensitivity test method for doing GSA was developed) talked about the dynamic nature of sensitivities. A simple chemical reaction was considered and the time-varying influence of the input uncertain parameters on it was presented. In another example, McCarthy et al. [11] studied the temporal dynamics of parameter sensitivities for gene expression in *Drosophila* embryos where they showed that influence of certain parameters like mRNA decay rate increased significantly over time while other parameters such as those related to transcription and translation decreased. These observations aligned with experimental results and allowed them to corroborate existing theories on the dynamic nature of gene expression in developing *Drosophila* embryos.

Cao et al. [14] looked at Sobol' Indices-based GSA for linear systems with parametric uncertainties and process noise for the first time. Analytical expressions for the evolution of only the first-order Sobol indices were derived and numerical examples where their analytical solutions aligned with Monte Carlo results were presented. However, the analytical expressions required indefinite symbolic integrals of impulse responses. This approach requires detailed knowledge of the linear model and its structure, which may not be discernible for all practical applications. The work in this paper, in contrast, presents a way to determine the Sobol' indices (first-order effects as well as higher order effects) while treating the stochastic linear model as a black box, thus

Contributed by the Design Engineering Division of ASME for publication in the Journal of Computational and Nonlinear Dynamics. Manuscript received May 29, 2018; final manuscript received September 21, 2018; published online January 7, 2019. Assoc. Editor: Paramsothy Jayakumar.

eliminating the need for exploiting the structure of the model in evaluating symbolic integrals.

This paper uses polynomial chaos (PC) to develop a surrogate probabilistic model for the stochastic linear system. PC is an uncertainty quantification tool, which has been used extensively in the literature to characterize the propagation of uncertainty through odes and pdes. It is shown in this work that an intrusive approach to determining PC coefficients is equivalent to differentially weighing several realizations of the stochastic system (similar to the stochastic collocation approach) when the system under analysis is linear and the uncertainties individually appear linearly in the model. This is done by assuming a novel set of bases, i.e., the Lagrange interpolation polynomials (LIPs) for the intrusive PC expansion, which has not been considered in the literature before. It allows one to develop an intrusive PC model nonintrusively for linear systems and makes evaluation of PC coefficients computationally cheaper.

After determining the PC probabilistic model, the pioneering work of Sudret [15] and Crestaux et al. [16] is used to derive the Sobol' indices at a negligible computational cost. Although PC has been used for GSA of linear dynamic systems before in Ref. [10], process noise as a disturbance to the model has never been considered. In this work, process noise is included while developing the PC model. Hence, when the Sobol' indices are derived, they reflect the contribution of the input parameters in the presence of process noise since the statistical information about the process noise is already embedded in them.

The outputs of interest in this paper are considered to be the first two moments of the stochastic system under the influence of Gaussian disturbance (or white process noise). The Sobol' indices associated with the mean represent the influence input model parameters have on the system when there is no disturbance. The indices associated with the second moment on the other hand represent how much the parameters influence our estimate of the variance of the states, i.e., we seek to characterize the source of uncertainty in the estimate of the variance (here, variance refers to variance due to process noise alone). The readers are encouraged to think in terms of figuring out how globally sensitive the variance estimate is to the uncertainty ranges of the model input parameters. Such an analysis is novel (to the authors' best knowledge) and forms the second major contribution of this paper.

The paper has been structured in the following way: Section 2 describes the systems of interest and the desired objective of the work. Section 3 provides an overview of Sobol' Indices. Section 4 presents the quantification of uncertainty propagation through time due to process noise and uncertain model parameters. This section also presents the equivalence of nonintrusive stochastic collocation-based polynomial chaos and the intrusive Galerkin projection approach. Section 5 presents results from literature on the determination of Sobol' indices from Polynomial Chaos coefficients. Section 6 applies the methods of the paper on two numerical examples for illustration. The paper finally terminates with concluding remarks in Sec. 7.

## 2 Problem Statement

Consider the continuous-time linear stochastic system of the form

$$\dot{\boldsymbol{x}} = A(\boldsymbol{\xi})\boldsymbol{x} + B(\boldsymbol{\xi})\boldsymbol{u} + G(\boldsymbol{\xi})\boldsymbol{w} \tag{1}$$

with initial conditions $\boldsymbol{x}(0) = \boldsymbol{x}_0(\boldsymbol{\xi})$, where $\boldsymbol{x} \in \mathbb{R}^n$ is the state vector of the system, $\boldsymbol{u} \in \mathbb{R}^m$ is the input vector, $\boldsymbol{w} \in \mathbb{R}^q$ is an additive noise term, and $\boldsymbol{\xi} \in \mathbb{R}^p$ is a vector of uncertain parameters. The uncertain parameter vector $\boldsymbol{\xi}$ is modeled as a time invariant random variable with a known probability distribution function (pdf). In this work, it is assumed that the pdf of $\boldsymbol{\xi}$ is uniform. It is also assumed that $\boldsymbol{w}(t)$ evolves according to a continuous white noise process with a probability measure given by

$$E_w[\boldsymbol{w}(t)] = 0 \tag{2}$$

$$E_w\left[\boldsymbol{w}(t_1)\boldsymbol{w}(t_2)^{\mathrm{T}}\right] = Q(\boldsymbol{\xi})\int_0^\infty \delta(t_1 - t_2)dt_1 \tag{3}$$

where $Q(\boldsymbol{\xi})$ denotes the parameter-dependent co-variance, $\delta(t)$ represents the Dirac delta function, and $E_w[\cdot]$ is the expectation operator evaluated over the $\boldsymbol{w}$ space.

The objective of this work is to determine and quantify the influence of the parameter vector $\boldsymbol{\xi}$ on the first two moments of the states ($\boldsymbol{\mu}$ and $\Sigma$) from a GSA perspective. The GSA is accomplished by calculating the popular variance-based measures called the Sobol' indices [17].

## 3 Sobol' Indices

The main objective of variance-based GSA techniques is to decompose the output variance of interest into a sum of variances contributed either by individual input parameters or by a combination of the input parameters.

For example, consider the scalar function

$$y = f(\boldsymbol{\xi}) \tag{4}$$

where $\boldsymbol{\xi} = [\xi_1, \ldots, \xi_p]^{\mathrm{T}}$ is the input parameter vector defined on the $p-$dimensional unit hypercube (i.e., $\boldsymbol{\xi} \in \Omega^p = [0,1]^p$) and $f(\boldsymbol{\xi})$ is integrable over $\Omega^p$.

The function in Eq. (4) can be decomposed (also known as the Sobol' decomposition) as

$$f(\xi_1, \ldots, \xi_p) = f_0 + \sum_{i=1}^{p} f_i(\xi_i) + \sum_{1\le i<j\le p} f_{ij}(\xi_i, \xi_j) + \cdots + f_{1,2,\ldots,p}(\xi_1, \ldots, \xi_p) \tag{5}$$

where $f_0$ is a constant and the integral of any of its summand $f_{i_1,\ldots,i_s}(\xi_{i_1}, \ldots, \xi_{i_s})$ over each of its independent variables is zero [15], i.e.,

$$\int_0^1 f_{i_1,\ldots,i_s}(\xi_{i_1}, \ldots, \xi_{i_s})d\xi_{i_k} = 0 \text{ for } 1 \le k \le s \tag{6}$$

Other properties of this decomposition (such as the number of terms in Eq. (5) or the orthogonality of $f_{i_1,\ldots,i_s}(\xi_{i_1}, \ldots, \xi_{i_s})$) can be found in Refs. [15] and [18], and have therefore not been included in this document.

It can be shown that, with the assumption of the properties listed in Ref. [15], the Sobol' decomposition is unique. In fact, the decomposition terms can be evaluated using the expressions

$$f_0 = \int_{\Omega^p} f(\boldsymbol{\xi})d\boldsymbol{\xi} \tag{7}$$

$$f_i(\xi_i) = \int_{\Omega^{p-1}} f(\boldsymbol{\xi})d\boldsymbol{\xi}_{\sim i} - f_0 \tag{8}$$

$$f_{ij}(\xi_i, \xi_j) = \int_{\Omega^{p-2}} f(\boldsymbol{\xi})d\boldsymbol{\xi}_{\sim\{ij\}} - f_0 - f_i(\xi_i) - f_j(\xi_j) \tag{9}$$

$$\vdots$$

where any summand can be expressed as the difference between a multidimensional integral and the previously evaluated summands. The operators $\int_{\Omega^{p-1}} d\boldsymbol{\xi}_{\sim i}$ and $\int_{\Omega^{p-2}} d\boldsymbol{\xi}_{\sim\{ij\}}$ in Eqs. (8) and (9) represent integrals over all variables except for $(\xi_i)$ and $(\xi_i, \xi_j)$, respectively. The notation used is identical to Ref. [15] and should be referred for more details.

Now, consider a stochastic variable $Y = f(\boldsymbol{\xi})$, which is dependent on an input random vector $\boldsymbol{\xi}$ where each element of $\boldsymbol{\xi}$ is uniformly distributed with a distribution $\xi_i \in U[0,1]$. The total variance of $Y$ can be then written as

$$D = \mathrm{var}[f(\boldsymbol{\xi})] = \int_{\Omega^p} f(\boldsymbol{\xi})^2 d\boldsymbol{\xi} - f_0^2 \tag{10}$$

Using the Sobol' decomposition of the function $f(\boldsymbol{\xi})$ and the orthogonal property of its summands, it can be shown that the total variance $D$ can be decomposed into

$$D = \sum_{i=1}^{p} D_i + \sum_{1 \le i < j \le p} D_{ij} + \cdots \tag{11}$$

where the partial variances $D_{i_1,\ldots,i_s}$ are defined as

$$D_{i_1,\ldots,i_s} = \int_{\Omega^s} f_{i_1,\ldots,i_s}(\xi_{i_1},\ldots,\xi_{i_s})^2 d\xi_{i_1},\ldots,d\xi_{i_s} \text{ for } 1 \le i_1 \le \cdots \le i_s \le p \text{ and } s = 1,\ldots,p \tag{12}$$

The Sobol' indices are eventually defined in terms of the partial variances as

$$S_{i_1,\ldots,i_s} = D_{i_1,\ldots,i_s}/D \tag{13}$$

Also, from Eq. (11), it easily follows that:

$$\sum_{i=1}^{p} S_i + \sum_{1 \le i < j \le p} S_{ij} + \cdots + S_{1,2,\ldots,p} = 1 \tag{14}$$

Hence, each index $S_{i_1,\ldots,i_s}$ represents the fraction of the total variance that is contributed by the combination of the uncertain parameters in the set $(\xi_1,\ldots,\xi_s)$. For example, $S_1$ would represent the fraction of the total variance contributed by the uncertainty in $\xi_1$ and $S_{12}$ would represent the fraction of the total variance contributed by the combined effects of the uncertainties in the random variables ($\xi_1$ and $\xi_2$).

In this work, the aim is to observe the time evolution of the Sobol' indices when the mean ($\boldsymbol{\mu}$) and the variance ($\Sigma$) of the states of a linear stochastic system with process noise are outputs of interest. That way, the global dependence of the $\boldsymbol{\mu}$ and $\Sigma$ on the uncertain parameters of the model $\boldsymbol{\xi}$ can be studied.

## 4 Propagation of Uncertainty Through Time

This section presents details on the development of a probabilistic model for the time evolution of the statistics (mean and variance) of the stochastic states of the system described in Eq. (1). The first step in the process is to quantify the propagation of uncertainty solely due to the process noise. This has been done extensively in the literature before and the necessary differential equations have been quoted in Sec. 4.1. The second step of the process is to quantify the propagation of uncertainty due to the uncertain parameters of the model. This is done by adopting a popular probabilistic modeling tool called polynomial chaos. The details of this step have been presented in Sec. 4.2.

**4.1 Propagation of Uncertainty Due to Process Noise.** It is well known that when white noise passes through a time invariant linear system, the pdf of the evolving state vector remains Gaussian and can hence be characterized completely by its first two moments. The differential equations that characterize this evolution are given by

$$\dot{\boldsymbol{\mu}} = A(\boldsymbol{\xi})\boldsymbol{\mu} + B(\boldsymbol{\xi})\boldsymbol{u} \tag{15}$$

$$\dot{\Sigma} = A(\boldsymbol{\xi})\Sigma + \Sigma A(\boldsymbol{\xi})^{\mathrm{T}} + G(\boldsymbol{\xi})Q(\boldsymbol{\xi})G(\boldsymbol{\xi})^{\mathrm{T}} \tag{16}$$

where $\boldsymbol{\mu}(t)$ and $\Sigma(t)$ represent the evolving mean and covariance of $\boldsymbol{x}(t)$. The initial condition for these equations is correspondingly given by

$$\boldsymbol{\mu}(0) = \boldsymbol{\mu}_0 = E_{\xi}[\boldsymbol{x}_0(\boldsymbol{\xi})] \tag{17}$$

$$\Sigma(0) = \Sigma_0 = E_{\xi}\left[(\boldsymbol{x}_0(\boldsymbol{\xi}) - \boldsymbol{\mu}_0)(\boldsymbol{x}_0(\boldsymbol{\xi}) - \boldsymbol{\mu}_0)^{\mathrm{T}}\right] \tag{18}$$

where $E_{\xi}[\cdot]$ is the expectation operator evaluated over the uncertain parameter $\boldsymbol{\xi}$ space.

Equations (15) and (16) are linear differential equations and can be grouped into the following linear system as:

$$\dot{z}(t,\boldsymbol{\xi}) = A_z(\boldsymbol{\xi})z + B_z(\boldsymbol{\xi})\boldsymbol{u}_z \tag{19}$$

where $z \in \mathbb{R}^{\tilde{n}}$ is defined by

$$z = \left[\boldsymbol{\mu}^{\mathrm{T}}, \Sigma_v^{\mathrm{T}}\right]^{\mathrm{T}}, \quad \Sigma_v = \mathrm{vec}[\Sigma], \quad \boldsymbol{u}_z = \left[\boldsymbol{u}^{\mathrm{T}}, 1\right]^{\mathrm{T}} \tag{20}$$

and $\tilde{n} = n + n^2$. The operator vec[·] in the above equation assembles columns of a matrix and stacks them vertically to make a vector of size equal to the number of elements in the matrix. A formal definition of vec[·] can be found in Ref. [19].

The matrices $A_z$ and $B_z$ in Eq. (19) are defined as

$$A_z = \begin{bmatrix} A & 0 \\ 0 & A_m \end{bmatrix}, A_m = A_m^{(1)} + A_m^{(2)}, A_m^{(1)} = I_n \otimes A, \tag{21}$$

$$A_m^{(2)} = \begin{bmatrix} I_n \otimes A(1,:) \\ I_n \otimes A(2,:) \\ \vdots \\ I_n \otimes A(n,:) \end{bmatrix} \text{ and } B_z = \begin{bmatrix} B & 0 \\ 0 & \mathrm{vec}\left[GQG^{\mathrm{T}}\right] \end{bmatrix} \tag{22}$$

where $A(i,:)$ refers to the $i$th row of $A$ and the operator $\otimes$ denotes the Kronecker product. Hence, Eq. (19) defines a stochastic linear system devoid of process noise, which is now only a function of the uncertain parameters, where the states represent the mean and the variance of $\boldsymbol{x}(t)$ due to process noise.

At this stage, although the uncertainty due to process noise has been quantified, the propagation of uncertainty due to the uncertain model parameters still needs to be worked out. Section 4.2 is directed at catering to model parameter uncertainties.

**4.2 Propagation of Uncertainty Due to Uncertain Model Parameters Using Polynomial Chaos.** Polynomial chaos has been an extremely popular tool in the literature for developing polynomial probabilistic models. It was first investigated by Norbert Wiener in his article [20] where he approximated states of a Gaussian process with an infinite series expansion with Hermite polynomials as bases. Subsequently, pioneering works by Cameron and Martin [21], Ghanem and Spanos [22] and Xiu and Karniadakis [23] have resulted in significant progress of PC concepts. It has allowed for the development of surrogate models, which can emulate the original stochastic system inexpensively and has been used to determine statistics (for example mean and variance) of states accurately. In this work, PC is used to develop a probabilistic model for stochastic linear systems as a stepping stone toward an efficient GSA.

From PC theory, the states of the system in Eq. (19) can be expressed as [24]

$$z(t,\boldsymbol{\xi}) = \sum_{i=1}^{\infty} z_{:,i}(t)\Psi_i(\boldsymbol{\xi}) \tag{23}$$

where $\Psi_i(\boldsymbol{\xi})$ is a complete set of multivariate orthogonal (with respect to the pdf of $\boldsymbol{\xi}$) polynomials and $z_{:,i} \in \mathbb{R}^{\tilde{n}}$ is the time-varying coefficient vector (i.e., $z_{:,i} = [z_{1,i} \cdots z_{\tilde{n},i}]^{\mathrm{T}}$) of $\Psi_i(\boldsymbol{\xi})$.

Depending on the desired level of accuracy, typically, the infinite series is truncated as an approximation

$$z(t,\xi) \approx \sum_{i=1}^{N} z_{:,i}(t)\Psi_i(\xi) \tag{24}$$

The objective here in this modeling technique is to evaluate the unknown vectors $z_{:,i}(t)$ over time. They can be determined by either intrusive methods or by nonintrusive methods [25]. Intrusive methods require an analytical knowledge of the system model while nonintrusive methods can treat models as black boxes. In this work, since the models of interest are linear, the intrusive Galerkin projection is considered and investigated.

On substituting Eq. (24) in Eq. (19), we get

$$\sum_{i=1}^{N} \dot{z}_{:,i}(t)\Psi_i(\xi) = A_z(\xi)\left[\sum_{i=1}^{N} z_{:,i}(t)\Psi_i(\xi)\right] + B_z(\xi)\boldsymbol{u}_z(t) \tag{25}$$

Taking the Galerkin Projection of Eq. (25) over the basis function space, a deterministic system of equations is derived

$$M_{PC}\dot{\boldsymbol{Z}}_{\boldsymbol{PC}} = A_{PC}\boldsymbol{Z}_{\boldsymbol{PC}} + B_{PC}\boldsymbol{u}_z(t) \tag{26}$$

where $\boldsymbol{Z}_{\boldsymbol{PC}} = \left[z_{:,1}^{\mathrm{T}},\ z_{:,2}^{\mathrm{T}}, \ldots,\ z_{:,N}^{T}\right]^{\mathrm{T}}$; $M_{\mathrm{PC}}$ is given by Eq. (28)

$$B_{\mathrm{PC}} = \begin{bmatrix} \langle B_{z(11)}, \Psi_1\rangle & \cdots & \langle B_{z(1p)}, \Psi_1\rangle \\ \vdots & \ddots & \vdots \\ \langle B_{z(\tilde{n}1)}, \Psi_1\rangle, & \cdots & \langle B_{z(\tilde{n}m)}, \Psi_1\rangle \\ \vdots & \ddots & \vdots \\ \langle B_{z(11)}, \Psi_N\rangle, & \cdots, & \langle B_{z(1p)}, \Psi_N\rangle \\ \vdots & \ddots & \vdots \\ \langle B_{z(\tilde{n}1)}, \Psi_N\rangle, & \cdots, & \langle B_{z(\tilde{n}m)}, \Psi_N\rangle \end{bmatrix}; \tag{27}$$

$$M_{\mathrm{PC}} = \begin{bmatrix} \langle\Psi_1,\Psi_1\rangle & 0_{\tilde{n}-2}^T & 0 & \langle\Psi_2,\Psi_1\rangle & 0_{\tilde{n}-2}^T & 0 & \cdots & \langle\Psi_N,\Psi_1\rangle & 0_{\tilde{n}-2}^T & 0 \\ 0 & \langle\Psi_1,\Psi_1\rangle & 0_{\tilde{n}-2}^T & 0 & \langle\Psi_2,\Psi_1\rangle & 0_{\tilde{n}-2}^T & \cdots & 0 & \langle\Psi_N,\Psi_1\rangle & 0_{\tilde{n}-1}^T \\ \vdots & \vdots & \vdots & \vdots & \vdots & \vdots & \ddots & \vdots & \vdots & \vdots \\ 0 & 0_{\tilde{n}-2}^T & \langle\Psi_1,\Psi_1\rangle & 0 & 0_{\tilde{n}-2}^T & \langle\Psi_2,\Psi_1\rangle & \cdots & 0 & 0_{\tilde{n}-1}^T & \langle\Psi_N,\Psi_1\rangle \\ \vdots & \vdots & \vdots & \vdots & \vdots & \vdots & \ddots & \vdots & \vdots & \vdots \\ \langle\Psi_1,\Psi_N\rangle & 0_{\tilde{n}-2}^T & 0 & \langle\Psi_2,\Psi_N\rangle & 0_{\tilde{n}-2}^T & 0 & \cdots & \langle\Psi_N,\Psi_N\rangle & 0_{\tilde{n}-2}^T & 0 \\ 0 & \langle\Psi_1,\Psi_N\rangle & 0_{\tilde{n}-2}^T & 0 & \langle\Psi_2,\Psi_N\rangle & 0_{\tilde{n}-2}^T & \cdots & 0 & \langle\Psi_N,\Psi_N\rangle & 0_{\tilde{n}-1}^T \\ \vdots & \vdots & \vdots & \vdots & \vdots & \vdots & \ddots & \vdots & \vdots & \vdots \\ 0 & 0_{\tilde{n}-2}^T & \langle\Psi_1,\Psi_N\rangle & 0 & 0_{\tilde{n}-2}^T & \langle\Psi_2,\Psi_N\rangle & \cdots & 0 & 0_{\tilde{n}-1}^T & \langle\Psi_N,\Psi_N\rangle \end{bmatrix} \tag{28}$$

$$A_{\mathrm{PC}} = \begin{bmatrix} \langle A_{z(11)}\Psi_1,\Psi_1\rangle, & \cdots & \langle A_{z(1\tilde{n})}\Psi_1,\Psi_1\rangle, & \langle A_{z(11)}\Psi_2,\Psi_1\rangle, & \cdots & \langle A_{z(1\tilde{n})}\Psi_2,\Psi_1\rangle, & \cdots, & \langle A_{z(11)}\Psi_N,\Psi_1\rangle, & \cdots & \langle A_{z(1\tilde{n})}\Psi_N,\Psi_1\rangle \\ \langle A_{z(21)}\Psi_1,\Psi_1\rangle, & \cdots & \langle A_{z(2\tilde{n})}\Psi_1,\Psi_1\rangle, & \langle A_{z(21)}\Psi_2,\Psi_1\rangle, & \cdots & \langle A_{z(2\tilde{n})}\Psi_2,\Psi_1\rangle, & \cdots, & \langle A_{z(21)}\Psi_N,\Psi_1\rangle, & \cdots & \langle A_{z(2\tilde{n})}\Psi_N,\Psi_1\rangle \\ \vdots & & & & & & & & & \\ & & \vdots & \vdots & & \vdots & & \vdots & & \vdots \\ \langle A_{z(\tilde{n}1)}\Psi_1,\Psi_1\rangle, & \cdots & \langle A_{z(\tilde{n}\tilde{n})}\Psi_1,\Psi_1\rangle, & \langle A_{z(\tilde{n}1)}\Psi_2,\Psi_1\rangle, & \cdots & \langle A_{z(\tilde{n}\tilde{n})}\Psi_2,\Psi_1\rangle, & \cdots, & \langle A_{z(\tilde{n}1)}\Psi_N,\Psi_1\rangle, & \cdots & \langle A_{z(\tilde{n}\tilde{n})}\Psi_N,\Psi_1\rangle \\ \langle A_{z(11)}\Psi_1,\Psi_2\rangle, & \cdots & \langle A_{z(1\tilde{n})}\Psi_1,\Psi_2\rangle, & \langle A_{z(11)}\Psi_2,\Psi_2\rangle, & \cdots & \langle A_{z(1\tilde{n})}\Psi_2,\Psi_2\rangle, & \cdots, & \langle A_{z(11)}\Psi_N,\Psi_2\rangle, & \cdots & \langle A_{z(1\tilde{n})}\Psi_N,\Psi_2\rangle \\ \vdots & & \vdots & \vdots & & \vdots & & \vdots & & \vdots \\ \langle A_{z(\tilde{n}1)}\Psi_1,\Psi_2\rangle, & \cdots & \langle A_{z(\tilde{n}\tilde{n})}\Psi_1,\Psi_2\rangle, & \langle A_{z(\tilde{n}1)}\Psi_2,\Psi_2\rangle, & \cdots & \langle A_{z(\tilde{n}\tilde{n})}\Psi_2,\Psi_2\rangle, & \cdots, & \langle A_{z(\tilde{n}1)}\Psi_N,\Psi_2\rangle, & \cdots & \langle A_{z(\tilde{n}\tilde{n})}\Psi_N,\Psi_2\rangle \\ \vdots & & \vdots & \vdots & & \vdots & & \vdots & & \vdots \\ \langle A_{z(11)}\Psi_1,\Psi_N\rangle, & \cdots & \langle A_{z(1\tilde{n})}\Psi_1,\Psi_N\rangle, & \langle A_{z(11)}\Psi_2,\Psi_N\rangle, & \cdots & \langle A_{z(1\tilde{n})}\Psi_2,\Psi_N\rangle, & \cdots, & \langle A_{z(11)}\Psi_N,\Psi_N\rangle, & \cdots & \langle A_{z(1\tilde{n})}\Psi_N,\Psi_N\rangle \\ \vdots & & \vdots & \vdots & & \vdots & & \vdots & & \vdots \\ \langle A_{z(\tilde{n}1)}\Psi_1,\Psi_N\rangle, & \cdots & \langle A_{z(\tilde{n}\tilde{n})}\Psi_1,\Psi_N\rangle, & \langle A_{z(\tilde{n}1)}\Psi_2,\Psi_N\rangle, & \cdots & \langle A_{z(\tilde{n}\tilde{n})}\Psi_2,\Psi_N\rangle, & \cdots, & \langle A_{z(\tilde{n}1)}\Psi_N,\Psi_N\rangle, & \cdots & \langle A_{z(\tilde{n}\tilde{n})}\Psi_N,\Psi_N\rangle \end{bmatrix} \tag{29}$$

and $A_{PC}$ is given by Eq. (29).

$M_{z(ij)}$ refers to the $i$th row $j$th column element of matrix $M_z$ and the operator $\langle g, h\rangle$ refers to the inner product operation

$$\langle g, h \rangle = \int_{\Omega^p} g(\boldsymbol{\xi}) h(\boldsymbol{\xi}) pdf(\boldsymbol{\xi}) d\boldsymbol{\xi} \tag{30}$$

where $\Omega^p$ is the support of $pdf(\boldsymbol{\xi})$ and is defined in Sec. 3. Solution to Eq. (26) yields the desired coefficients.

In existing literature, the traditional choice for the PC bases $\Psi_i(\boldsymbol{\xi})$ has been to select orthogonal polynomials according to the Wiener Askey scheme [23]. However, the authors explore an alternate set of bases in this work called the Lagrange interpolation polynomials. This unique selection of bases leads to significant advantages to intrusive PC modeling and form an integral part of this paper's contribution.

Lagrange interpolation polynomials have been extensively used in the approximation theory literature to develop surrogate polynomial models of systems or functions where a finite set of discrete observations are available [26]. The bases are constructed such that the surrogate model inherently replicates the value of the system at the observation points. This strategy ensures that the error in modeling at those points is zero, which may be a desired property in some applications.

In fact, LIP has also been used to develop PC models under the stochastic collocation framework of nonintrusive PC [27]. However, to the authors' best knowledge, the possibility of using LIPs as bases while doing intrusive PC has never been investigated. In this paper, such an arrangement is explored for the first time. It is seen that when LIPs are employed as the choice of bases, a decoupled PC system is obtained, which eventually leads to extremely efficient computation of intrusive Galerkin projection-based PC coefficients by eliminating the need to evaluate multivariate integrals in Eqs. (27)–(29).

The choice of collocation points for the LIP is made in a manner identical to [27] (see Gaussian abscissas in the Tensor product quadrature rules section of Ref. [27]). These points are derived after taking tensor products of sets of univariate Gauss quadrature points where each set of points depend on the pdf of the uncertain variable. For example, if in the problem of interest there are two independent uncertain variables $\xi_1$ and $\xi_2$ and they are both uniformly distributed as $\xi_1, \xi_2 \in U(-1, 1)$: the collocation points are simply the grid nodes obtained from the tensor product of Gauss-Legendre quadrature points.

Using the above strategy to select the collocation points make the LIP bases orthogonal to each other with respect to the pdf of the uncertain variables. For example, consider a case where $\xi_1$ and $\xi_2$ are two independent random variables. If $L_{ij}$ are the LIPs defined via

$$L_{ij}(\xi_1, \xi_2) = \left( \prod_{p=1, i \neq p}^{n_1} \frac{\left(\xi_1 - \xi_1^{(p)}\right)}{\left(\xi_1^{(i)} - \xi_1^{(p)}\right)} \right) \left( \prod_{q=1, j \neq q}^{n_2} \frac{\left(\xi_2 - \xi_2^{(q)}\right)}{\left(\xi_2^{(j)} - \xi_2^{(q)}\right)} \right) \tag{31}$$

then it can be shown that they are orthogonal to each other with respect to the joint pdf of $\xi_1$ and $\xi_2$, i.e.,

$$\langle L_{pq}, L_{rs} \rangle = \begin{cases} c_{pq} & p = r \text{ and } q = s \\ 0 & \text{otherwise} \end{cases} \tag{32}$$

where $c_{pq}$ are constants, $\xi_1^{(\cdot)}$ and $\xi_2^{(\cdot)}$ are the quadrature points in the $\xi_1$ and $\xi_2$ directions, respectively, and $n_1$ and $n_2$ are the number of quadrature points in the $\xi_1$ and $\xi_2$ directions, respectively.

When $p = r$ and $q = s$

$$\langle L_{pq}, L_{pq} \rangle = 0.25 \int_{-1}^{1} \int_{-1}^{1} L_{pq}(\xi_1, \xi_2)^2 d\xi_1 d\xi_2 \tag{33}$$

Note that $L_{pq}^2$ is a polynomial function in $\xi_1$ and $\xi_2$ having highest orders of $2n_1 - 2$ and $2n_2 - 2$, respectively. Gaussian quadrature rules allow the perfect evaluation of the aforementioned integral via a weighted sum of function evaluations. A tensor product of $n_1$ and $n_2$ quadrature points is sufficient to do so as they allow a polynomial of order up to $2n_1 - 1$ and $2n_2 - 1$ to be integrated without error. As the polynomial order of interest ($L_{pq}^2$) is less, we can write

$$\langle L_{pq}, L_{pq} \rangle = \sum_{i=1}^{n_1} \sum_{j=1}^{n_2} w_{ij} L_{pq}\left(\xi_1^{(i)}, \xi_2^{(j)}\right)^2 \tag{34}$$

where $w_{ij}$ are the Gaussian quadrature weights. Recognizing that

$$L_{pq}\left(\xi_1^{(i)}, \xi_2^{(j)}\right) = \begin{cases} 1 & i = p \text{ and } j = q \\ 0 & \text{otherwise} \end{cases} \tag{35}$$

we get

$$\langle L_{pq}, L_{pq} \rangle = w_{pq} \tag{36}$$

This inherent property of LIP bases to have a value of 1 at only one of the grid points (Eq. (35)) is henceforth referred to as the *zero error property*. The zero error property is why LIPs are so popular in the approximation theory community.

With a development similar to the one above, it can be shown that when $p \neq r$ or $q \neq s$ we have

$$\langle L_{pq}, L_{rs} \rangle = 0 \tag{37}$$

Although this property of orthogonality has been shown only for a two-dimensional case, it can be easily extended to higher dimensions of uncertainties.

The zero error and the orthogonality property can be used to now show that if LIPs are used as basis functions in a PC expansion for an uncertain linear system where the uncertain variables also occur linearly individually (i.e., the partial derivative with respect to a variable of the multilinear term is independent of that variable), then the desired PC coefficients determined via the intrusive Galerkin Projection are specific realizations of the original system.

Once again, an illustration on a linear system with two uncertain independent variables has been presented, although the development can easily be extended to any dimensions of uncertainties.

Similar to Eq. (19), let a linear system be of the form

$$\dot{\boldsymbol{z}} = A_z(\xi_1, \xi_2)\boldsymbol{z} + B_z(\xi_1, \xi_2)\boldsymbol{u_z} \tag{38}$$

where the basis functions are chosen to be the LIP (defined in Eq. (31)). A finite PC expansion leads to

$$\boldsymbol{z} \approx \sum_{i=1}^{n_1} \sum_{j=1}^{n_2} \boldsymbol{Z_{ij}}(t) L_{ij}(\xi_1, \xi_2) \tag{39}$$

Equation (39) is then substituted in Eq. (38) to get

$$\sum_{i=1}^{n_1} \sum_{j=1}^{n_2} \dot{\boldsymbol{Z}}_{\boldsymbol{ij}} L_{ij}(\xi_1, \xi_2) = A_z(\xi_1, \xi_2) \left( \sum_{i=1}^{n_1} \sum_{j=1}^{n_2} \boldsymbol{Z_{ij}} L_{ij}(\xi_1, \xi_2) \right) + B_z(\xi_1, \xi_2)\boldsymbol{u_z} \tag{40}$$

Taking the Galerkin Projection of Eq. (40) on the basis function space yields a series of deterministic equations, which can be solved to yield the coefficients $\boldsymbol{Z_{ij}}(t)$. In the interest of brevity, the derivation of the deterministic system pertinent to the Galerkin projection of Eq. (40) only on the first basis function is shown. The other systems can be derived in an identical fashion.

The inner product of Eq. (40) with $L_{11}$ leads to

$$\sum_{i=1}^{n_1} \sum_{j=1}^{n_2} \dot{\boldsymbol{Z}}_{\boldsymbol{ij}} \langle L_{ij}, L_{11} \rangle = \left[ \sum_{i=1}^{n_1} \sum_{j=1}^{n_2} \langle \left(A_z(\xi_1, \xi_2)\boldsymbol{Z_{ij}}\right) L_{ij}(\xi_1, \xi_2), L_{11} \rangle \right] + \langle B_z(\xi_1, \xi_2), L_{11} \rangle \boldsymbol{u_z} \tag{41}$$

The orthogonality property can be used to determine that the left-hand side of Eq. (41) is

$$w_{11}\dot{\boldsymbol{Z}}_{\boldsymbol{11}} \tag{42}$$

If the system matrix $A_z(\xi_1, \xi_2)$ is linear or bilinear in $\xi_1$ and $\xi_2$, the integrand in the first inner product integral (on the right-hand side of Eq. (41)) is a polynomial with highest order $2n_1 - 1$ and $2n_2 - 1$ with respect to $\xi_1$ and $\xi_2$, respectively. Hence, a $n_1 n_2$ point quadrature rule can be used to perfectly evaluate those integrals. Since those quadrature points are the same as the ones selected to generate the LIP bases, the zero error property of LIP can be used to show that the right-hand side of Eq. (41) is given by

$$w_{11}A_z\left(\xi_1^{(1)}, \xi_2^{(1)}\right)\boldsymbol{Z}_{\boldsymbol{11}} + w_{11}B_z\left(\xi_1^{(1)}, \xi_2^{(1)}\right)\boldsymbol{u}_{\boldsymbol{z}} \tag{43}$$

leading to the deterministic system

$$w_{11}\dot{\boldsymbol{Z}}_{\boldsymbol{11}} = w_{11}A_z\left(\xi_1^{(1)}, \xi_2^{(1)}\right)\boldsymbol{Z}_{\boldsymbol{11}} + w_{11}B_z\left(\xi_1^{(1)}, \xi_2^{(1)}\right)\boldsymbol{u}_{\boldsymbol{z}} \tag{44}$$

$$\Rightarrow \dot{\boldsymbol{Z}}_{\boldsymbol{11}} = A_z\left(\xi_1^{(1)}, \xi_2^{(1)}\right)\boldsymbol{Z}_{\boldsymbol{11}} + B_z\left(\xi_1^{(1)}, \xi_2^{(1)}\right)\boldsymbol{u}_{\boldsymbol{z}} \tag{45}$$

Hence, it is evident that the PC coefficients ($\boldsymbol{Z}_{\boldsymbol{11}}(t)$) of the basis function $L_{11}$ are simply given by a system realization of the original system at the quadrature point $\left(\xi_1^{(1)}, \xi_2^{(1)}\right)$. This result also extends to the other deterministic systems derived from the Galerkin projections. To remain consistent with the notation in Eq. (24), the double indexing strategy (Eq. (39)) is now relinquished to adopt a single index addressing. This can be done as follows:

Let a matrix $M_L$ be defined comprising all the bases

$$M_L = \begin{bmatrix} L_{11} & \cdots & L_{1n_2} \\ \vdots & \ddots & \vdots \\ L_{n_1 1} & \cdots & L_{n_1 n_2} \end{bmatrix} \tag{46}$$

The single indexing can be then defined such that the elements of $M_L$ are assimilated row wise into a single indexed vector as follows:

$$\Psi = [L_{11}, \ldots, L_{1n_2}, \ldots, L_{n_1 1}, \ldots, L_{n_1 n_2}]^{\mathrm{T}} \tag{47}$$

where $\Psi_i$ represents the $i$th element basis function of $\Psi$. The corresponding coefficient vectors ($\boldsymbol{Z}_{\boldsymbol{ij}}(t)$) are addressed in a similar manner such that $\boldsymbol{z}_{:,i}(t)$ refers to the coefficient vector of $\Psi_i$. It should be pointed out that the surrogate models obtained via traditional PC—Galerkin and LIP blending of system realizations are identical, i.e., they lead to the same exact surrogate model.

The result obtained in Eq. (45) leads to a remarkably simple composition of matrices $M_{\mathrm{PC}}$, $A_{\mathrm{PC}}$, and $B_{\mathrm{PC}}$ as illustrated in the following equations:

$$M_{\mathrm{PC}} = \begin{bmatrix} w_{11}I_{\tilde{n}} & 0_{\tilde{n}} & \cdots & 0_{\tilde{n}} \\ 0_{\tilde{n}} & w_{12}I_{\tilde{n}} & \cdots & 0_{\tilde{n}} \\ \vdots & \vdots & \ddots & \vdots \\ 0_{\tilde{n}} & 0_{\tilde{n}} & \cdots & w_{n_1 n_2}I_{\tilde{n}} \end{bmatrix} \tag{48}$$

$$B_{\mathrm{PC}} = \begin{bmatrix} w_{11}B_z\left(\xi_1^{(1)}, \xi_2^{(1)}\right) \\ w_{12}B_z\left(\xi_1^{(1)}, \xi_2^{(2)}\right) \\ \vdots \\ w_{n_1 n_2}B_z\left(\xi_1^{(n_1)}, \xi_2^{(n_2)}\right) \end{bmatrix} \tag{49}$$

$$A_{\mathrm{PC}} = \begin{bmatrix} w_{11}A_z\left(\xi_1^{(1)}, \xi_2^{(1)}\right) & 0_{\tilde{n}} & \cdots & 0_{\tilde{n}} \\ 0_{\tilde{n}} & w_{12}A_z\left(\xi_1^{(1)}, \xi_2^{(2)}\right) & \cdots & 0_{\tilde{n}} \\ \vdots & \vdots & \ddots & \vdots \\ 0_{\tilde{n}} & 0_{\tilde{n}} & \cdots & w_{n_1 n_2}A_z\left(\xi_1^{(n_1)}, \xi_2^{(n_2)}\right) \end{bmatrix} \tag{50}$$

Although the impact of this result may remain unclear at the outset, it actually has profound implications from a computational perspective. Previously, to obtain a PC surrogate model using intrusive Galerkin projection methods, several definite integrals needed evaluation (over the compact uncertain domain) to obtain the set of deterministic odes for the coefficients. This task of evaluating symbolic integrations often makes it extremely difficult or in some cases impossible to derive the PC system. This development shows that since the intrusive Galerkin method is equivalent to Lagrange interpolation blending, the definite integrals over the uncertain space need not be carried out at all to obtain the equivalent surrogate model. Instead, the true system just needs to be evaluated at a certain specific set of points and the PC approximate model is simply a differential weighing of these realizations: providing a cook book formula to obtain intrusive PC surrogate models easily without the need of exercising Galerkin Projections.

To keep a consistency in notation and make the previous development more generic, the following sets are now defined:

$$S = \{\boldsymbol{\xi} | \boldsymbol{\xi} = \left[\xi_1^{(i_1)}, \ldots, \xi_p^{(i_p)}\right]^{\mathrm{T}}, 1 \le i_j \le n_j, 1 \le j \le p\} \tag{51}$$

where $S$ represents the set of all quadrature node points. Every element of the $S$ is $\in \mathbb{R}^p$ holding the co-ordinates of the quadrature points. $i_1$ through $i_p$ are indices to count through all the grid node points and $n_j$ represents the number of grid points in the $\xi_j$ direction. Since the total number of grid points is the tensor product of the quadrature points in each direction, the number of elements in the set $S$ is

$$N = \prod_{i=1}^{p} n_i \tag{52}$$

The generic multivariate LIP can be defined as

$$L_{i_1,\ldots,i_p}(\boldsymbol{\xi}) = \prod_{k=1}^{p}\left(\prod_{j=1, i_k \neq j}^{n_k}\left(\frac{\left(\xi_k - \xi_k^{(j)}\right)}{\left(\xi_k^{(i_k)} - \xi_k^{(j)}\right)}\right)\right) \tag{53}$$

such that

$$L_{i_1,\ldots,i_p}(\boldsymbol{\xi}) = \begin{cases} 1 & \text{for } \boldsymbol{\xi} = \left[\xi_1^{(i_1)}, \ldots, \xi_p^{(i_p)}\right]^{\mathrm{T}} \\ 0 & \text{for } \xi_1 \neq \xi_1^{(i_1)} \text{ or } \xi_2 \neq \xi_2^{(i_2)} \\ & \text{or } \cdots \xi_m \neq \xi_p^{(i_p)} \end{cases} \tag{54}$$

Equation (54) represents the zero error property.

We define another set $L_b$ to hold all the basis functions

$$L_b = \{\Psi | \Psi = L_{i_1,\ldots,i_p}(\boldsymbol{\xi}), 1 \le i_j \le n_j, 1 \le j \le p\} \tag{55}$$

The cardinality of $L_b$ is the same as the cardinality of $S$. In fact, each basis function in $L_b$ is equal to 1 when evaluated at one particular element in $S$ and is equal to 0 when evaluated at all other grid points in set $S$. Therefore, each grid point in $S$ has a corresponding basis function in $L_b$.

Elements in $S$ and $L_b$ are arranged in a matrix ($\Xi$) and a vector ($\Psi$), respectively, for convenience of communication, i.e.,

$$\Xi = \left[\boldsymbol{\xi}^{(1)}, \boldsymbol{\xi}^{(2)}, \ldots, \boldsymbol{\xi}^{(N)}\right] \tag{56}$$

where $\Xi \in \mathbb{R}^{p\times N}$, $\boldsymbol{\xi}^{(i)} \in S$ and

$$\Psi = [\Psi_1, \Psi_2, \ldots, \Psi_N]^{\mathrm{T}} \tag{57}$$

where $\Psi_i \in L_b$ and

$$\Psi_i\left(\boldsymbol{\xi}^{(j)}\right) = \begin{cases} 1 & \text{for } i = j \\ 0 & \text{for } i \neq j \end{cases} \tag{58}$$

Using the notation above, and recalling once again that the coefficients of a model where the bases are LIPs are simply the model realizations at the grid points, we get the final surrogate model expression as

$$z(t, \boldsymbol{\xi}) \approx \sum_{i=1}^{N} z\left(t, \boldsymbol{\xi}^{(i)}\right)\Psi_i \tag{59}$$

**4.3 Numerical Example.** To illustrate how the methods presented above can be implemented, an application on a simple spring mass damper linear system is shown. The governing differential equation is given by

$$m\ddot{x} + c\dot{x} + kx = du \tag{60}$$

where $m$ is the mass, $k$ is the spring constant, $c$ is the damping constant, $d$ is the control influence gain, and $x$ is the displacement of the mass.

The state space realization of the system is given by

$$\begin{bmatrix} \dot{x}_1 \\ \dot{x}_2 \end{bmatrix} = \begin{bmatrix} 0 & 1 \\ -k/m & -c/m \end{bmatrix}\begin{bmatrix} x_1 \\ x_2 \end{bmatrix} + \begin{bmatrix} 0 \\ 1/m \end{bmatrix} u \tag{61}$$

We assume, for illustrative purposes, that $k$ and $c$ are uncertain, independent, and have uniform distributions

$$k \in U[12, 28] \text{ and } c \in U[0.7, 1.3] \tag{62}$$

If two standard uniformly distributed random variables are defined as $\boldsymbol{\xi} = [\xi_1, \xi_2]^{\mathrm{T}}$ where

$$\xi_1 \in U[-1, 1] \text{ and } \xi_2 \in U[-1, 1] \tag{63}$$

then the system parameters can be expressed as

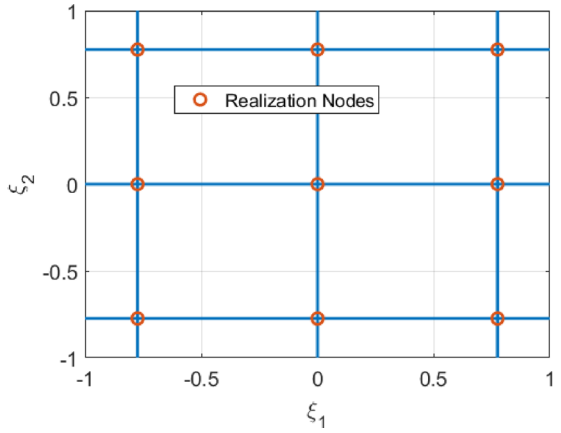


**Fig. 1 PC realization nodes for $n_1 = n_2 = 3$**

$$k = k_0 + k_1\xi_1 \text{ and } c = c_0 + c_1\xi_2 \tag{64}$$

where $k_0 = 20$, $k_1 = 8$, $c_0 = 1$, and $c_1 = 0.3$. Note that for this example, $\tilde{n} = 2$ and $p = 2$.

The first step in deriving the surrogate model is to assume a degree of approximation. The degree of approximation is dependent on the number of quadrature points that are selected in each direction of uncertainty. Considering there are two uncertain variables, two sets of quadrature points are selected in their corresponding directions. For illustration, we select an equal number of points for $\xi_1$ as well as $\xi_2$ (although this is not a necessity) i.e., $n_1 = 3$ and $n_2 = 3$. The points in each direction are given by

$$\xi_1^{(1)} = \frac{-15^{1/2}}{5};\ \xi_1^{(2)} = 0;\ \xi_1^{(3)} = \frac{15^{1/2}}{5} \tag{65}$$

and

$$\xi_2^{(1)} = \frac{-15^{1/2}}{5};\ \xi_2^{(2)} = 0;\ \xi_2^{(3)} = \frac{15^{1/2}}{5} \tag{66}$$

These points are actually the roots of an $(n_1 + 1)$th order Legendre polynomial and hence, are also the univariate Gauss–Legendre points. Both sets of points have the same magnitudes since both uncertain variables have identical distributions.

A tensor product of the univariate quadrature points now yields the desired comprehensive set of collocation points or grid points. The total number of grid points is given by $N = n_1 \times n_2 = 9$ (see Eq. (52)). Similar to Eq. (56), the points are assembled in a single matrix $\Xi$ shown in Eq. (67) where the $i$th column ($\boldsymbol{\xi}^{(i)}$) represents the $i$th grid point. These points are also presented as circles in the $\xi_1$, $\xi_2$ uncertain space in Fig. 1

$$\Xi = \begin{bmatrix} \frac{-15^{1/2}}{5} & \frac{-15^{1/2}}{5} & \frac{-15^{1/2}}{5} & 0 & 0 & 0 & \frac{15^{1/2}}{5} & \frac{15^{1/2}}{5} & \frac{15^{1/2}}{5} \\ \frac{-15^{1/2}}{5} & 0 & \frac{15^{1/2}}{5} & \frac{-15^{1/2}}{5} & 0 & \frac{15^{1/2}}{5} & \frac{-15^{1/2}}{5} & 0 & \frac{15^{1/2}}{5} \end{bmatrix} \tag{67}$$

The final step of developing the surrogate model is to assimilate the matrix $\Psi$, which holds the LIP bases. These bases can be generated using Eq. (53). $N = 9$ basis functions are generated using the relation

$$L_{i_1,i_2}(\boldsymbol{\xi}) = \prod_{k=1}^{m=2}\left(\prod_{j=1, i_k\neq j}^{n_k}\left(\frac{\left(\xi_k - \xi_k^{(j)}\right)}{\left(\xi_k^{(i_k)} - \xi_k^{(j)}\right)}\right)\right) \tag{68}$$

The bases are assimilated into the vector $\Psi$ where

$$\Psi = [L_{1,1}, L_{1,2}, L_{1,3}, L_{2,1}, L_{2,2}, L_{2,3}, L_{3,1}, L_{3,2}, L_{3,3}]^{\mathrm{T}} \tag{69}$$

Note that the $i$th element basis function of $\Psi$ is referenced as $\Psi_i$.

The final surrogate model can be written as Eq. (59) where $z(t, \boldsymbol{\xi}) = [x_1(t, \boldsymbol{\xi}), x_2(t, \boldsymbol{\xi})]^{\mathrm{T}}$.

## 5 Evaluation of Sobol' Indices From Polynomial Chaos

Sudret [15] and Crestaux et al. [16] showed that once a probabilistic model is available for a stochastic output of interest via PC, the Sobol' indices could be evaluated from the PC coefficients for a negligible computational cost. In fact, the information of the fractional variance contribution by each individual uncertain input parameter is already embedded and evaluated while calculating the PC coefficients. Hence, simple algebraic expressions of the PC coefficients can be derived to map them to the Sobol' indices.

In contrast to Refs. [15] and [16] where the polynomial bases used was the traditional family of orthogonal polynomials given by the Wiener–Askey scheme, in this work, results from these articles are used to derive the Sobol' indices directly from the LIP-based PC coefficients. In order to use their results, it is necessary to transform the probabilistic model derived in Eq. (59) (where the bases are LIPs) to another model such that the bases are given by an orthogonal family of polynomials aligned with the Wiener–Askey schematic.

This two-step process has been elaborated in this section.

**5.1 Transformation of Bases.** Let the new set of orthogonal polynomial bases be denoted by $\Theta(\boldsymbol{\xi}) = [\theta_0(\boldsymbol{\xi}), \theta_1(\boldsymbol{\xi}), \ldots, \theta_{N-1}(\boldsymbol{\xi})]^{\mathrm{T}}$ where $\theta_i$ represents the $(i+1)$th element of $\Theta$. We seek a transformation, i.e., a set of coefficients $\boldsymbol{r}_{:,i}(t)$ such that

$$z(t,\boldsymbol{\xi}) \approx \sum_{i=1}^{N} \boldsymbol{z}_{:,i}(t)\Psi_i(\boldsymbol{\xi}) = \sum_{i=0}^{N-1} \boldsymbol{r}_{:,i}(t)\theta_i(\boldsymbol{\xi}) \tag{70}$$

Since the order of the polynomials in both the expansions remains the same, the transformation is unique and linear. It can be represented using the following relation:

$$\begin{bmatrix} \boldsymbol{r}_{:,0}(t)^{\mathrm{T}} \\ \boldsymbol{r}_{:,1}(t)^{\mathrm{T}} \\ \vdots \\ \boldsymbol{r}_{:,N-1}(t)^{\mathrm{T}} \end{bmatrix} = M_b \begin{bmatrix} \boldsymbol{z}_{:,1}(t)^{\mathrm{T}} \\ \boldsymbol{z}_{:,2}(t)^{\mathrm{T}} \\ \vdots \\ \boldsymbol{z}_{:,N}(t)^{\mathrm{T}} \end{bmatrix} \tag{71}$$

where $M_b \in \mathbb{R}^{N\times N}$ is a mapping matrix, which depends on the selection of $\Theta$ and is given by

$$M_b = \begin{bmatrix} \Theta\left(\boldsymbol{\xi}^{(1)}\right)^{\mathrm{T}} \\ \Theta\left(\boldsymbol{\xi}^{(2)}\right)^{\mathrm{T}} \\ \vdots \\ \Theta\left(\boldsymbol{\xi}^{(N)}\right)^{\mathrm{T}} \end{bmatrix}^{-1} \underbrace{\begin{bmatrix} \Psi\left(\boldsymbol{\xi}^{(1)}\right)^{\mathrm{T}} \\ \Psi\left(\boldsymbol{\xi}^{(2)}\right)^{\mathrm{T}} \\ \vdots \\ \Psi\left(\boldsymbol{\xi}^{(N)}\right)^{\mathrm{T}} \end{bmatrix}}_{M_c} \tag{72}$$

However, recognizing the property of LIP bases where they have a value of 1 at their corresponding collocation point and a value of 0 at the other collocation points, we get $M_c = I_N$ and Eq. (72) reduces to

$$M_b = \begin{bmatrix} \Theta\left(\boldsymbol{\xi}^{(1)}\right)^{\mathrm{T}} \\ \Theta\left(\boldsymbol{\xi}^{(2)}\right)^{\mathrm{T}} \\ \vdots \\ \Theta\left(\boldsymbol{\xi}^{(N)}\right)^{\mathrm{T}} \end{bmatrix}^{-1} \tag{73}$$

Once the PC coefficients $\boldsymbol{r}_{:,i}(t)$ corresponding to the Wiener Askey family of orthogonal polynomials is available, the Sobol' indices can be directly calculated using results in Ref. [15].

**5.2 Calculation of Sobol' Indices.** For ease of communication to the reader, let us consider that only the first element of $z(t,\boldsymbol{\xi})$ is the output of interest. It should be noted that this consideration is in no way a limitation since the development on the first state can be easily extended to the other states in an identical fashion. Hence, in this subsection, we interest ourselves with the PC expansion of the scalar quantity $z_1(t,\boldsymbol{\xi})$, which is given by

$$z_1(t,\boldsymbol{\xi}) = \sum_{i=0}^{N-1} r_{1,i}(t)\theta_i(\boldsymbol{\xi}) \tag{74}$$

where $r_{1,i}(t)$ represents the first element of $\boldsymbol{r}_{:,i}(t)$.

Due to the orthogonality of $\theta_i(\boldsymbol{\xi})$, it can be shown that the mean and the total variance of $z_1(t,\boldsymbol{\xi})$ are given by

$$\bar{z}_1 = E_{\boldsymbol{\xi}}[z_1(t,\boldsymbol{\xi})] = r_{1,0}(t) \tag{75}$$

$$D_{\mathrm{PC}}^{(1)} = \mathrm{var}\left[\sum_{i=0}^{N-1} r_{1,i}(t)\theta_i(\boldsymbol{\xi})\right] = \sum_{i=1}^{N-1} r_{1,i}^2(t) E_{\boldsymbol{\xi}}\left[\theta_i(\boldsymbol{\xi})^2\right] \tag{76}$$

The superscript $^{(1)}$ in $D_{\mathrm{PC}}^{(1)}$ has been introduced to identify that $D_{\mathrm{PC}}^{(1)}$ corresponds to the total variance of the first state $z_1(t,\boldsymbol{\xi})$. Similarly, the total variance of the $i$th state $z_i(t,\boldsymbol{\xi})$ would be represented by $D_{\mathrm{PC}}^{(i)}$.

Following the development in Ref. [15], the Sobol' indices for $z_1(t,\boldsymbol{\xi})$ are given by:

$$S_{\mathrm{PC}(i_1,\ldots,i_s)}^{(1)} = \sum_{\boldsymbol{\alpha}\in\mathbb{P}_{i_1,\ldots,i_s}} r_{1,\boldsymbol{\alpha}}^2(t) E_{\boldsymbol{\xi}}\left[\theta_{\boldsymbol{\alpha}}(\boldsymbol{\xi})^2\right] / D_{\mathrm{PC}}^{(1)} \tag{77}$$

where $\boldsymbol{\alpha} = [\alpha_1, \ldots, \alpha_p]$, a tuple, is used to represent a particular basis function and

$$\mathbb{P}_{i_1,\ldots,i_s} = \left\{ \boldsymbol{\alpha}: \begin{array}{llll} \alpha_k > 0 & \forall k = 1,\ldots,p, & k \in (i_1,\ldots,i_s) \\ \alpha_j = 0 & \forall k = 1,\ldots,p, & k \notin (i_1,\ldots,i_s) \end{array} \right\} \tag{78}$$

In summary, $\mathbb{P}_{i_1,\ldots,i_s}$ represents a set with indices (or $\boldsymbol{\alpha}$), which correspond only to polynomials, which are functions of $(\xi_{i_1},\ldots,\xi_{i_s})$. For example, $\mathbb{P}_2$ would represent a set of indices, which correspond to a subset of $\Theta$ where $\theta_i$ is only a function of $\xi_2$ and not any other $\xi_i$. Similarly, $\mathbb{P}_{1,2,3}$ would represent a set of indices, which correspond to a subset of $\Theta$ where $\theta_i$ is only a function of $(\xi_1,\xi_2,\xi_3)$ and not any other $\xi_i$.

Hence, in Eq. (77), depending on the desired Sobol' index (or the joint fractional contribution to total variance by a combination of inputs), the value of the index is evaluated by first assimilating all the PC coefficients corresponding to a subset of all the bases, which are *only* a function of those inputs. These selected coefficients are then squared, summed, and divided by $D_{\mathrm{PC}}^{(1)}$.

The Sobol' indices for all the other states ($S_{\mathrm{PC}(i_1,\ldots,i_s)}^{(2)}$, $S_{\mathrm{PC}(i_1,\ldots,i_s)}^{(3)}$,…) of $z(t,\boldsymbol{\xi})$ can be determined in an identical way by defining appropriate variables ($D_{\mathrm{PC}}^{(2)}$, $D_{\mathrm{PC}}^{(3)}$, …). These values represent the fractional contribution to the total variance of $z(t,\boldsymbol{\xi})$. Since $z(t,\boldsymbol{\xi})$ holds the elements of $\boldsymbol{\mu}$ and $\Sigma$, we can now easily observe which model parameter uncertainties have the most influence on the evolution of $\boldsymbol{\mu}$ and $\Sigma$.

The Sobol' indices corresponding to $\boldsymbol{\mu}$ represent the fractional contribution of variance in $\boldsymbol{x}(t,\boldsymbol{\xi})$ by the model parameters if process noise was absent, since the dynamic equations of $\boldsymbol{\mu}$ are identical to the noise free system. These indices are $S_{\mathrm{PC}(i_1,\ldots,i_s)}^{(j)}$ for $j = [1,\ldots,n]$.

The Sobol' indices corresponding to $\Sigma$ represent the fractional contribution of variance in the *variance estimate of* $\boldsymbol{x}(t,\boldsymbol{\xi})$ *due to process noise*. To simplify, the proposed amalgamation of techniques allows us to evaluate and quantify the uncertainty (and its source of contribution) in the variance of a linear system with process noise. These indices are $S_{\mathrm{PC}(i_1,\ldots,i_s)}^{(j)}$ for $j = [n+1,\ldots,n+n^2]$.

## 6 Numerical Examples

In order to illustrate the proposed methodology, two numerical examples have been presented in this section. The first example

involves regulating the position of a hovering helicopter under wind disturbances and the second example studies the motion of the sprung mass of a quarter car model under uncertain road disturbances.

**6.1 Regulation of a Hovering Helicopter.** The example of a hovering helicopter under wind disturbance as well as model parameter uncertainties [24,28] is considered. The dynamics of the system are given by

$$\dot{\boldsymbol{x}} = A\boldsymbol{x} + B\delta + B_w u_w \tag{79}$$

where $\boldsymbol{x} = [u_h, q_h, \theta_h, y]^{\mathrm{T}}$

$$A = \begin{bmatrix} p_1 & p_2 & -g & 0 \\ p_3 & p_4 & 0 & 0 \\ 0 & 1 & 0 & 0 \\ 1 & 0 & 0 & 0 \end{bmatrix}, \quad B = \begin{bmatrix} p_5 \\ p_6 \\ 0 \\ 0 \end{bmatrix} \quad \text{and} \quad B_w = \begin{bmatrix} -p_1 \\ -p_3 \\ 0 \\ 0 \end{bmatrix} \tag{80}$$

$u_h(ft/s)$ represents the horizontal velocity of the helicopter, $\theta_h(\times 10^{-2}\,\mathrm{rad})$ represents the pitch angle, $q_h(\times 10^{-2}\,\mathrm{rad/s})$ represents the pitch angular velocity, and $y(ft)$ represents the horizontal perturbation from a ground point reference. $g$ corresponds to the acceleration due to gravity and is equal to 0.322. $\delta$ represents the control input to the system. $u_w$ represents the wind disturbance on the helicopter and is modeled as a zero mean Gaussian white noise with variance $\sigma_w^2 = 18$.

The model comprises of six model parameters ($p_1$–$p_6$). $p_1$–$p_4$ represent the aerodynamic stability derivatives while the parameters $p_5$ and $p_6$ represent the aerodynamic control derivatives.

Initial conditions to the system are assumed to be deterministic and are adopted from [24]

$$\boldsymbol{x}_0 = [0.7929, -0.0466, -0.1871, 0.5780]^{\mathrm{T}} \tag{81}$$

The control law implemented is that of a full state feedback [24] where

$$\delta = -K\boldsymbol{x} \tag{82}$$

and $K = [1.9890, -0.2560, -0.7589, 1]$. On substituting the control law in the original system, we get the closed-loop stochastic system

$$\dot{\boldsymbol{x}} = A_c\boldsymbol{x} + B_w u_w \tag{83}$$

where $A_c = A - BK$. Similar to Ref. [24], it is assumed that parameters $\boldsymbol{p} = [p_1,\ p_2,\ p_3,\ p_4]^{\mathrm{T}}$ are uncertain and are modeled as uniform distributions within the bounds

$$\boldsymbol{p}_{lb} = [-0.0488, 0.0013, 0.126, -3.3535]^{\mathrm{T}} \tag{84}$$

$$\boldsymbol{p}_{ub} = [-0.0026, 0.0247, 2.394, -0.1765]^{\mathrm{T}} \tag{85}$$

The first step in the analysis is to determine the order of PC expansion desired. The order determines the fidelity of the probabilistic model: higher the order, higher is the fidelity. Considering there are four uncertain parameters, we can choose a distinct order of expansion in each direction of the uncertain space. The order of expansion in each direction also determines the number of collocation points that are needed in each direction. For illustrative purposes, we assume an equal order of expansion in each direction (i.e., $n_{\mathrm{PC}} = 3$) leading to an equal number of collocation points in each direction: $n_1 = n_2 = n_3 = n_4 = n_o = 4$ where $n_i$ represents the number of collocation in the direction of $p_i$. The co-ordinates of the collocation points can be evaluated according to Sec. 4.2.

Since the total number of collocation points are given by a tensor product of the collocation points in each direction, we get (for this problem), $N = 4^4 = 256$. Therefore, we have 256 corresponding LIP basis functions. After realizing the moment equations at the 256 collocation points, we develop the probabilistic model with LIPs as bases. Using an appropriate transformation matrix $M_b$, the model is transformed to one where the bases are now multivariate Legendre polynomials. The coefficients of these Legendre polynomials are assimilated, squared, and summed to determine the Sobol' indices for each element in $\boldsymbol{\mu}(t)$ and $\Sigma(t)$.

Since there are four uncertain parameters, the total number of indices are $2^p - 1 = 15$. They are arranged in the following order:

$$\boldsymbol{S}(t) = [S_1, S_2, S_3, S_4, S_{12}, S_{13}, S_{14}, S_{23}, S_{24}, S_{34}, S_{123}, S_{124}, S_{134}, S_{234}, S_{1234}]^{\mathrm{T}} \tag{86}$$

where the subscript indices of $S$ correspond to the index of the parameters in $\boldsymbol{p}$.

Figures 2 and 3 present the time evolution of the indices. Figure 2 caters to $\boldsymbol{\mu}$ while Fig. 3 caters to the diagonal elements of $\Sigma$. The diagonal elements of $\Sigma$ were chosen to be presented since they represent the variance of each element of $\boldsymbol{x}$. Similar results for the cross-covariance terms can also be derived. However, they have not been included in this document.

The indices have been plotted as bands in the figures. From Eq. (14), we already know that the sum of all the indices should add up to one and this is evident when all the bands are stacked on top of each other. Although there are a total of 15 indices under analysis, only a prominent few bands are visibly distinguishable which have the most influence. For example, in Fig. 2(*a*), which represents the Sobol' indices for the mean horizontal velocity of the helicopter, $S_1, S_2, S_3, S_4, S_{14}, S_{24}$, and $S_{34}$ indices are most prominent. This indicates that the total variance of the mean value of the horizontal velocity of the helicopter is mainly contributed by parameters $p_1, p_2, p_3, p_4$ individually and coupled influences from $(p_1, p_4)$, $(p_2, p_4)$ and $(p_3, p_4)$. Similar results are also seen for the other elements of $\boldsymbol{\mu}$ in Figs. 2(*b*)–2(*d*). However, on observing the width of the band for $S_4$, it is quite evident that the uncertainty in $p_4$ contributes the most toward the total variance of $\boldsymbol{\mu}$.

It is also interesting to note that $S_4$ is no longer the dominant contributor to the total variance when we look at $\Sigma$. We see that for $\Sigma$, the uncertainty in $p_3$ is most significant. Not only is $p_3$ significant alone, its contribution in conjunction with $p_4$ (for $\Sigma_{2,2}$ and $\Sigma_{3,3}$) as well as $p_1$ (for $\Sigma_{4,4}$) is significant.

Hence, we can conclude from Figs. 2 and 3 that it will serve the manufacturer to invest more resources in determining the values of $p_3$ and $p_4$ more accurately, i.e., reduce the uncertainty associated with them to reduce the uncertainty in the total variance.

**6.2 Quarter Car Model.** The second example considered is that of a quarter car [29,30]. A schematic figure of the quarter car model is shown in Fig. 4.

The model dynamics are given by

$$\dot{\boldsymbol{x}} = A_q\boldsymbol{x} + B_q h \tag{87}$$

where $\boldsymbol{x} = [x_1, x_2, \dot{x}_1, \dot{x}_2]^{\mathrm{T}}$,

$$A_q = \begin{bmatrix} 0 & 0 & 1 & 0 \\ 0 & 0 & 0 & 1 \\ -\dfrac{k_1}{m_1} - \dfrac{k_2}{m_1} & \dfrac{k_2}{m_1} & -\dfrac{c}{m_1} & \dfrac{c}{m_1} \\ \dfrac{k_2}{m_2} & -\dfrac{k_2}{m_2} & \dfrac{c}{m_2} & -\dfrac{c}{m_2} \end{bmatrix} \quad \text{and} \quad B_q = \begin{bmatrix} 0 \\ 0 \\ \dfrac{k_1}{m_1} \\ 0 \end{bmatrix} \tag{88}$$

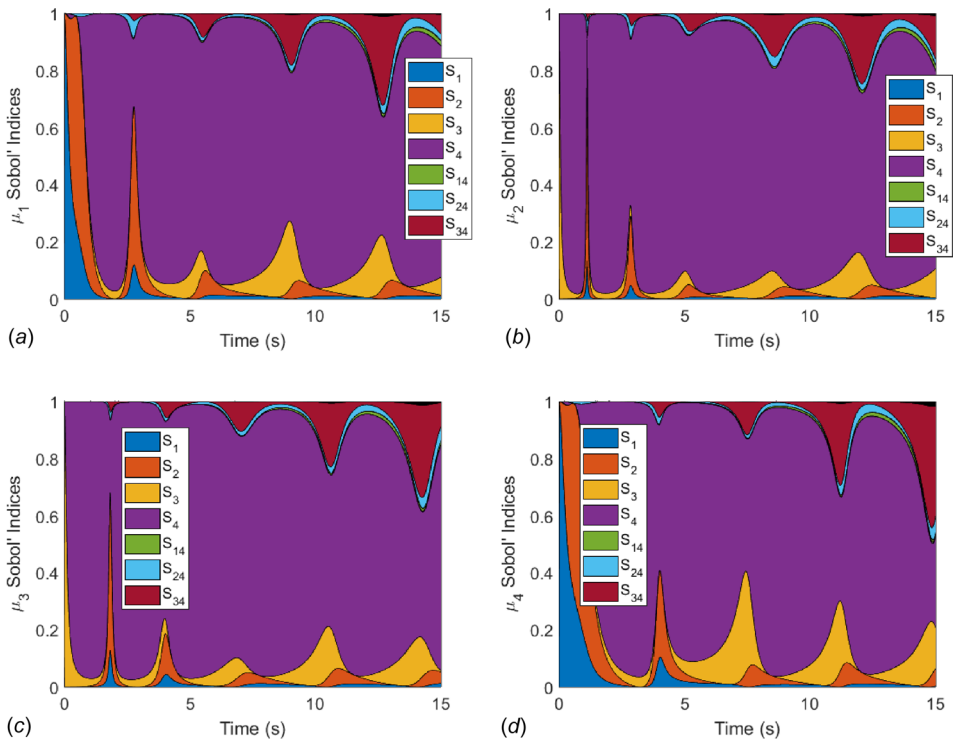


**Fig. 2 Evolution of Sobol' indices corresponding to the diagonal elements of $\mu$ over time: (*a*) $\mu_1$, (*b*) $\mu_2$, (*c*) $\mu_3$, and (*d*) $\mu_4$**

$m_1$ represents the unsprung mass, $m_2$ is the sprung mass, $k_1$ is the stiffness of the tire, $k_2$ is the stiffness of the suspension, and $c$ is the damping constant of the suspension.

The model above is used to represent the vertical motion of the quarter car. It is assumed in this work that the car moves in the horizontal direction with a constant velocity $V = 10\,\mathrm{m/s}$. The road dynamics $h(t)$ is derived from Ref. [31] and is modeled as colored noise. The governing equation is given by

$$\dot{h} = -aVh + w(t) \tag{89}$$

where $a$ is a parameter, which determines road quality, $V$ is the velocity of the car, and $w(t)$ is a white noise process with the co-

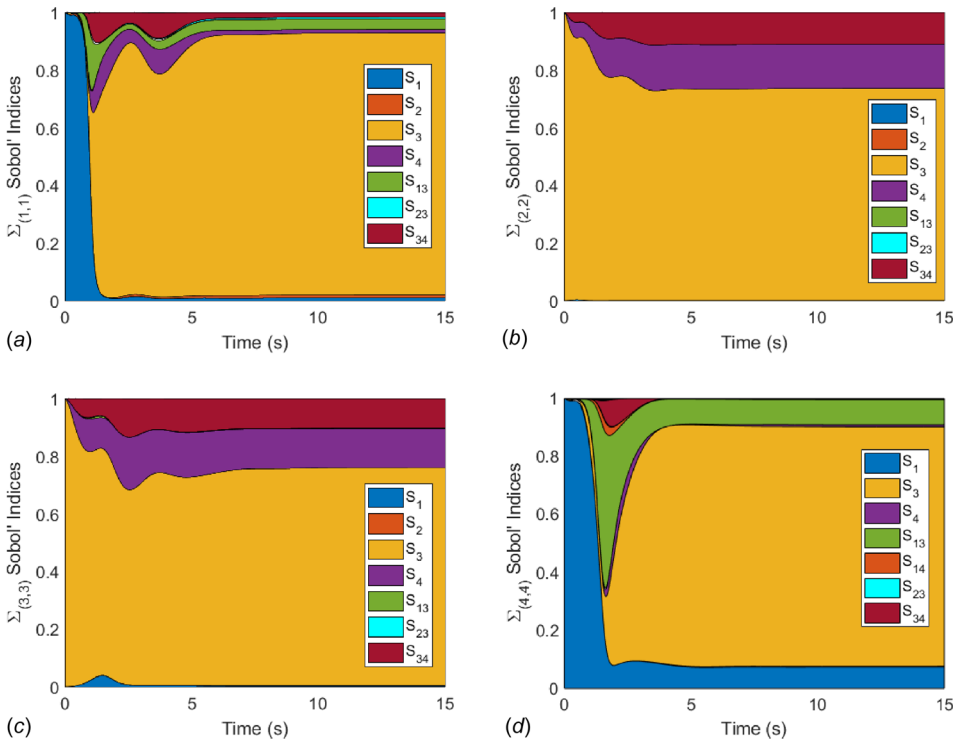


**Fig. 3 Evolution of Sobol' indices corresponding to the diagonal elements of $\Sigma$ over time: (*a*) $\Sigma_{(1,1)}$, (*b*) $\Sigma_{(2,2)}$, (*c*) $\Sigma_{(3,3)}$, and (*d*) $\Sigma_{(4,4)}$**

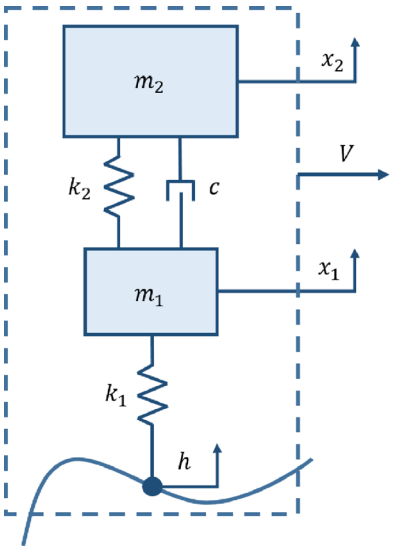


**Fig. 4 Schematic diagram of the quarter car model**

variance function $\sigma_w^2 = 2\sigma^2 aV$. The value of $\sigma^2$ is fixed at $9 \times 10^{-6}\text{m}^2$ and is taken from literature [31].

On augmenting the road dynamics, the stochastic system becomes

$$\dot{\boldsymbol{x}} = A\boldsymbol{x} + Bw(t) \tag{90}$$

where

$$A = \begin{bmatrix} 0 & 0 & 1 & 0 & 0 \\ 0 & 0 & 0 & 1 & 0 \\ -\frac{k_1}{m_1} - \frac{k_2}{m_1} & \frac{k_2}{m_1} & -\frac{c}{m_1} & \frac{c}{m_1} & \frac{k_1}{m_1} \\ \frac{k_2}{m_2} & -\frac{k_2}{m_2} & \frac{c}{m_2} & -\frac{c}{m_2} & 0 \\ 0 & 0 & 0 & 0 & -aV \end{bmatrix} \text{ and } B = \begin{bmatrix} 0 \\ 0 \\ 0 \\ 0 \\ 1 \end{bmatrix} \tag{91}$$

In this work, it is assumed that the spring constants, damping constant, and the road condition are uncertain (i.e., $\boldsymbol{p} = [p_1,\ p_2,\ p_3,\ p_4]^{\mathrm{T}} = [k_1,\ k_2,\ c,\ a]^{\mathrm{T}}$). The nominal values of these uncertain parameters are taken from literature [30,31]. They are then assumed to be uniformly distributed within a $\pm 30\%$ variation about their nominal values. This leads to a lower and an upper bound of

$$\boldsymbol{p}_{lb} = [84000, 17500, 700, 0.105]^{\mathrm{T}} \tag{92}$$

$$\boldsymbol{p}_{ub} = [156000, 32500, 1300, 0.195]^{\mathrm{T}} \tag{93}$$

The masses have values $m_1 = 31\,\text{kg}$ and $m_2 = 229\,\text{kg}$ [30]. It is assumed for all simulations that the unsprung mass ($m_1$) has an initial displacement of 5 mm and all other states are at their mean position, i.e., the system is simulated with initial conditions given by

$$\boldsymbol{x}_0 = [0.005, 0, 0, 0, 0]^{\mathrm{T}} \tag{94}$$

Note that, in this problem, the variance of the white noise is a linear function of an uncertain model parameter ($a$) and hence is also a random variable. However, this does not pose an issue in the analysis and the problem is approached in a manner similar to the previous one.

Once again, the number of collocation points chosen in each direction of uncertainty is kept the same at a value of $n_1 = n_2 = n_3 = n_4 = n_o = 4$. Considering there are four uncertainties, we get $N = 256$ LIP bases and their corresponding 256 collocation points. On running the stochastic linear model at these collocation points, the LIP bases coefficients are determined. $M_b$ is then used to transform them to a probabilistic model with multivariate Legendre polynomials as bases (since the distribution of the uncertain parameters are all uniform). Similar to the previous problem, the coefficients from the new model are then used to evaluate the desired Sobol' indices for $\boldsymbol{\mu}(t)$ and $\Sigma(t)$. The arrangement of the indices is done as per Eq. (86).

Since the major concern in this problem is to monitor the vertical displacement of the car chassis, we are only interested in the state $x_2(t)$. Hence, Sobol' indices corresponding to only $\mu_2$ and $\Sigma_{(2,2)}$ are presented.

Figures 5 and 6 are used to present the Sobol' indices for the variables of interest. Figure 5 shows the indices for the mean of the chassis displacement while Fig. 6 shows the indices for the variance of the chassis displacement. It is once again evident from the figures that different parameters have influence over the total variance when different outputs of interest are considered. We see that for $\mu_2$, the total variance is initially largely dependent on the uncertainty of $p_2$. However, with time, this influence wanes and the uncertainty due to the combination of $(p_1, p_2, p_3)$ starts dominating.

For $\Sigma_{(2,2)}$, we see that at initial stages, $p_4$ has most influence but its dominance is overwhelmed by $p_1$ and $p_2$ with time. It is also interesting to see that the individual influences of all the parameters $p_1$ through $p_4$ count for most part of the total variance and joint contribution for the parameters is only minimal as seen from the indices ($S_{12}$,$S_{13}$,$S_{14}$,$S_{23}$ and $S_{24}$).

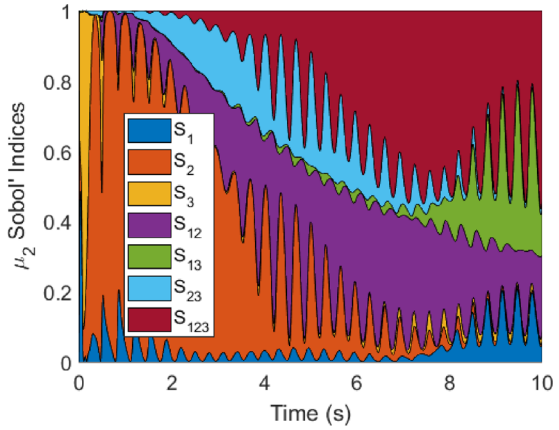


**Fig. 5 Sobol' indices for $\mu_2$**

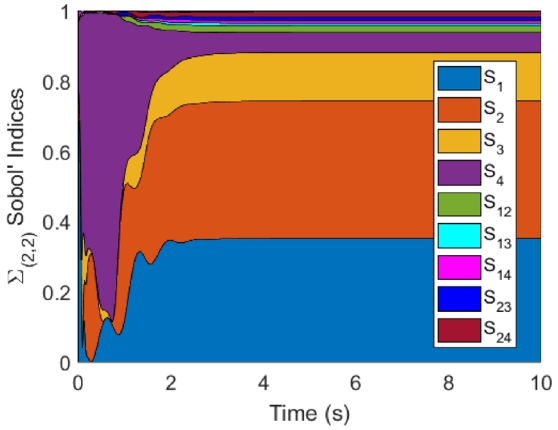


**Fig. 6 Sobol' indices for $\Sigma_{(2,2)}$**

## 7 Conclusions

This paper has presented an approach to develop Polynomial Chaos models of linear stochastic systems without the necessity to evaluate any indefinite integrals, which has been a drawback of intrusive polynomial chaos. It is shown that intrusive polynomial chaos is identical to stochastic collocation (provided the uncertain variables appear multilinearly) as long as Lagrange interpolation polynomials are used as bases. The coefficients from these models are then used to determine Sobol indices for the outputs of interest.

The paper also investigates the case when the outputs of interest are the mean and the co-variance of linear systems under the influence of process noise. It is observed that for a system, it is not necessary that the predominant contributor to the uncertainty in the mean and the variance be due to the same model input parameters. Hence, investing appropriate resources in lowering uncertainties in appropriate parameters are contingent on the choice of the output. It is often necessary in the forecasting frameworks to have a good estimate of the variance in the presence of process noise. If the same system is plagued with model parameter uncertainties, it then becomes important to know what factors contribute most to the uncertainty in the estimate of those variances. The methodology presented in this paper allows one to do that.

It should be noted, however, that the method is subjected to the curse of dimensionality where the number of collocation points exponentially increases with the number of uncertain variables (similar to basic multivariate stochastic collocation). This requires increasing computational efforts to compute the said coefficients and could be prohibitive for large-scale uncertainties. However, a future scope of work could entail looking into sparse grid collocation points (as opposed to tensor product LIP based) to reduce computational burden with increasing uncertainties.


## Acknowledgment

This material is based on the work supported through National Science Foundation (NSF) under Awards No. CMMI- 1537210. All results and opinions expressed in this paper are those of the authors and do not reflect opinions of NSF.

## Funding Data

- National Science Foundation (CMMI-1537210).


## References


[1] Kalman, R. E., 1960, "A New Approach to Linear Filtering and Prediction Problems," J. Basic Eng., **82**(1), pp. 35–45.

[2] Julier, S., Uhlmann, J., and Durrant-Whyte, H. F., 2000, "A New Method for the Nonlinear Transformation of Means and Covariances in Filters and Estimators," IEEE Trans. Automatic Control, **45**(3), pp. 477–482.

[3] Adurthi, N., Singla, P., and Singh, T., 2018, "Conjugate Unscented Transformation: Applications to Estimation and Control," ASME J. Dyn. Syst., Meas., Control, **140**(3), p. 030907.

[4] Evensen, G., 2003, "The Ensemble Kalman Filter: Theoretical Formulation and Practical Implementation," Ocean Dyn., **53**(4), pp. 343–367.

[5] Houtekamer, P. L., and Mitchell, H. L., 1998, "Data Assimilation Using an Ensemble Kalman Filter Technique," Mon. Weather Rev., **126**(3), pp. 796–811.

[6] Saltelli, A., Ratto, M., Tarantola, S., and Campolongo, F., 2006, "Sensitivity Analysis Practices: Strategies for Model-Based Inference," Reliab. Eng. Syst. Saf., **91**(10–11), pp. 1109–1125.

[7] Cho, K.-H., Shin, S.-Y., Kolch, W., and Wolkenhauer, O., 2003, "Experimental Design in Systems Biology, Based on Parameter Sensitivity Analysis Using a Monte Carlo Method: A Case Study for the TNFα-Mediated NF-κ B Signal Transduction Pathway," Simulation, **79**(12), pp. 726–739.

[8] Rodriguez-Fernandez, M., Kucherenko, S., Pantelides, C., and Shah, N., 2007, "Optimal Experimental Design Based on Global Sensitivity Analysis," *Computer Aided Chemical Engineering*, Vol. 24, Elsevier, Amsterdam, The Netherlands, pp. 63–68.

[9] Lamboni, M., Monod, H., and Makowski, D., 2011, "Multivariate Sensitivity Analysis to Measure Global Contribution of Input Factors in Dynamic Models," Reliab. Eng. Syst. Saf., **96**(4), pp. 450–459.

[10] Sandoval, E. H., Anstett-Collin, F., and Basset, M., 2012, "Sensitivity Study of Dynamic Systems Using Polynomial Chaos," Reliab. Eng. Syst. Saf., **104**, pp. 15–26.

[11] McCarthy, G. D., Drewell, R. A., and Dresch, J. M., 2015, "Global Sensitivity Analysis of a Dynamic Model for Gene Expression in Drosophila Embryos," Peer J., **3**, p. e1022.

[12] McRae, G. J., Tilden, J. W., and Seinfeld, J. H., 1982, "Global Sensitivity Analysis—A Computational Implementation of the Fourier Amplitude Sensitivity Test (FAST)," Comput. Chem. Eng., **6**(1), pp. 15–25.

[13] Drignei, D., and Mourelatos, Z. P., 2012, "Parameter Screening in Statistical Dynamic Computer Model Calibration Using Global Sensitivities," ASME J. Mech. Des., **134**(8), p. 081001.

[14] Cao, J., Du, F., and Ding, S., 2013, "Global Sensitivity Analysis for Dynamic Systems With Stochastic Input Processes," Reliab. Eng. Syst. Saf., **118**, pp. 106–117.

[15] Sudret, B., 2008, "Global Sensitivity Analysis Using Polynomial Chaos Expansions," Reliab. Eng. Syst. Saf., **93**(7), pp. 964–979.

[16] Crestaux, T., Le Maitre, O., and Martinez, J.-M., 2009, "Polynomial Chaos Expansion for Sensitivity Analysis," Reliab. Eng. Syst. Saf., **94**(7), pp. 1161–1172.

[17] Archer, G., Saltelli, A., and Sobol, I., 1997, "Sensitivity Measures, Anova-Like Techniques and the Use of Bootstrap," J. Stat. Comput. Simul., **58**(2), pp. 99–120.

[18] Homma, T., and Saltelli, A., 1996, "Importance Measures in Global Sensitivity Analysis of Nonlinear Models," Reliab. Eng. Syst. Saf., **52**(1), pp. 1–17.

[19] Horn, R. A., Horn, R. A., and Johnson, C. R., 1990, *Matrix Analysis*, Cambridge University Press, Cambridge, UK.

[20] Wiener, N., 1938, "The Homogeneous Chaos," Am. J. Math., **60**(4), pp. 897–936.

[21] Cameron, R. H., and Martin, W. T., 1947, "The Orthogonal Development of Non-Linear Functionals in Series of Fourier-Hermite Functionals," Ann. Math., **48**(2), pp. 385–392.

[22] Ghanem, R. G., and Spanos, P. D., 1991, "Stochastic Finite Elements: A Spectral Approach," *Stochastic Finite Elements: A Spectral Approach*, Springer, New York.

[23] Xiu, D., and Karniadakis, G. E., 2002, "The Wiener—Askey Polynomial Chaos for Stochastic Differential Equations," SIAM J. Sci. Comput., **24**(2), pp. 619–644.

[24] Konda, U., Singla, P., Singh, T., and Scott, P. D., 2011, "State Uncertainty Propagation in the Presence of Parametric Uncertainty and Additive White Noise," ASME J. Dyn. Syst., Meas., Control, **133**(5), p. 051009.

[25] Kim, K.-K. K., Shen, D. E., Nagy, Z. K., and Braatz, R. D., 2013, "Wiener's Polynomial Chaos for the Analysis and Control of Nonlinear Dynamical Systems with Probabilistic Uncertainties," IEEE Control Syst., **33**(5), pp. 58–67.

[26] Xiu, D., 2010, *Numerical Methods for Stochastic Computations: A Spectral Method Approach*, Princeton University Press, Princeton, NJ.

[27] Eldred, M., and Burkardt, J., 2009, "Comparison of Non-Intrusive Polynomial Chaos and Stochastic Collocation Methods for Uncertainty Quantification," AIAA Paper No. AIAA 2009-976.

[28] Bryson, A. E., and Mills, R. A., 1998, "Linear-Quadratic-Gaussian Controllers with Specified Parameter Robustness," J. Guid., Control, Dyn., **21**(1), pp. 11–18.

[29] Yue, C., Butsuen, T., and Hedrick, J., 1989, "Alternative Control Laws for Automotive Active Suspensions," ASME J. Dyn. Syst., Meas., Control, **111**(2), pp. 286–291.

[30] Gobbi, M., Levi, F., and Mastinu, G., 2006, "Multi-Objective Stochastic Optimisation of the Suspension System of Road Vehicles," J. Sound Vib., **298**(4–5), pp. 1055–1072.

[31] Narayanan, S., and Senthil, S., 1998, "Stochastic Optimal Active Control of a 2-DOF Quarter Car Model With Non-Linear Passive Suspension Elements," J. Sound Vib., **211**(3), pp. 495–506.